

Published in final edited form as:

Oncogene. 2011 April 7; 30(14): 1631–1642. doi:10.1038/onc.2010.547.

Combining epitope-distinct antibodies to HER2: cooperative inhibitory effects on invasive growth

A. Emde¹, C-R. Pradeep¹, DA. Ferraro¹, N. Ben-Chetrit¹, M. Sela², B. Ribba³, Z. Kam⁴, and Y. Yarden¹

¹Department of Biological Regulation, The Weizmann Institute of Science, Rehovot, Israel

²Department of Immunology, The Weizmann Institute of Science, Rehovot, Israel

³INRIA Rhône-Alpes, Project-team NUMED, Ecole Normale Supérieure de Lyon, Lyon, France

⁴Department of Molecular Cell Biology, The Weizmann Institute of Science, Rehovot, Israel

Abstract

Monoclonal antibodies (mAbs) to HER2 are currently used to treat breast cancer, but low clinical efficacy, along with primary and acquired resistance to therapy, commonly limit clinical applications. We previously reported that combinations of antibodies directed at non-overlapping epitopes of HER2 are endowed with enhanced antitumor effects, probably due to accelerated receptor degradation. Here, we extend these observations to three-dimensional mammary cell models, and compare the effects of single mAbs with the effects of antibody combinations. Collectively, our *in vitro* assays and computational image analyses indicate that combining mAbs against different epitopes of HER2 better inhibits invasive growth. Importantly, while growth factors are able to reduce intraluminal apoptosis and induce an invasive phenotype, combinations of mAbs better than single mAbs can reverse the growth factor-induced phenotypes of HER2-overexpressing spheroids. In conclusion, our studies propose that mAb combinations negate the biological effects of growth factors on invasive growth of HER2-overexpressing cells. Hence, combining mAbs offers a therapeutic strategy, potentially able to enhance clinical efficacy of existing antireceptor immuno-therapeutics.

Keywords

breast cancer; growth factor; trastuzumab; tyrosine kinase; 3D culture

Introduction

The ErbB family of receptor tyrosine kinases consists of four members. Upon activation by a ligand, such as epidermal growth factor (EGF), the receptors form hetero- and homodimers able to signal along downstream pathways, such as the phosphoinositide-3-kinase/AKT pathway and several mitogen-activated protein kinase pathways, such as the extracellular signal-regulated kinase (Yarden and Sliwkowski, 2001). Excessive ErbB signaling plays crucial roles in the progression of human epithelial malignancies. In the past decade, several treatments have been developed to target the ErbB signaling network (Baselga, 2006).

© 2011 Macmillan Publishers Limited All rights reserved

Correspondence: Professor Y Yarden, Department of Biological Regulation, The Weizmann Institute of Science, Candiotty Building (room 302), 1 Hertzl Street, Rehovot 76100, Israel. yosef.yarden@weizmann.ac.il.

Conflict of interest

The authors declare no conflict of interest.

Nevertheless, certain features of this receptor family, such as redundancy and complexity of signaling, limit efficacy of targeted therapy (Citri and Yarden, 2006). The *ErbB-2/HER2* proto-oncogene is amplified in 25–30% of human primary breast tumors (Slamon *et al.*, 1987). Moreover, HER2 overexpression/amplification was observed with high frequencies also in lung, gastric and oral cancers (Schneider *et al.*, 1989; Yoshida *et al.*, 1989; Weiner *et al.*, 1990; Hou *et al.*, 1992; Xia *et al.*, 1997). An effective drug targeting HER2 is the humanized antibody trastuzumab, also known as Herceptin (Lemieux *et al.*, 2009). Despite clinical efficacy, the majority of trastuzumab-treated patients, who initially respond to trastuzumab therapy, develop resistance within 1 year. Therefore, mechanisms of action and processes underlying resistance are of high interest (Nahta and Esteva, 2006).

In need of circumventing resistance, new therapeutic strategies have been developed. One emerging drug is the dual tyrosine kinase inhibitor lapatinib, targeting both ErbB-1/EGF receptor (EGFR) and HER2 (Xia *et al.*, 2002). Another important candidate is the monoclonal antibody (mAb) pertuzumab, which inhibits heterodimerization of HER2 (Agus *et al.*, 2002). Yet another promising strategy combines mAbs against the same receptor. Our previous studies revealed that HER2 comprises several antigenic sites; one of the most immunogenic epitopes mediates heterodimerization (Klapper *et al.*, 1997). We later reported that pairs of mAbs specific to distinct epitopes of HER2, of which one is involved in heterodimerization, are highly effective in inhibiting tumorigenic growth (Ben-Kasus *et al.*, 2009). The strategy of combining two or more antibodies against distinct epitopes of the same receptor was shown previously (Drebin *et al.*, 1988; Kasprzyk *et al.*, 1992), and its added benefit has been attributed to various factors, including enhanced receptor degradation (Friedman *et al.*, 2005), improved recruitment of immune effector cells (Spiridon *et al.*, 2002) and prevention of the formation of an active fragment of HER2 (Scheuer *et al.*, 2009). It is notable that pairwise combinations of non-competitive antibodies to EGFR similarly enhance receptor degradation and synergistically inhibit cancer cell growth (Friedman *et al.*, 2005; Pedersen *et al.*, 2010; Spangler *et al.*, 2010). In addition, a recent clinical trial, which combined trastuzumab and pertuzumab in patients with HER2-positive breast cancer, whose disease had progressed during previous trastuzumab-based therapy, achieved a 24.2% objective response rate (Baselga *et al.*, 2009).

This study aimed at the establishment of an *in vitro* model system able to reflect quantitatively cooperative effects of monoclonal anti-HER2 antibodies. To this end, we employed human breast cancer cell lines, as well as an engineered normal mammary cell line, monocyte chemoattractant factor 10A (MCF10A), overexpressing HER2. When tested under conditions permitting mammary cells to form duct-like spheroids in extracellular matrix, combinations of anti-HER2 mAbs negated an invasive phenotype promoted by growth factors. Computational image analyses attributed the inhibitory action of mAb combinations to an ability to induce lumen formation and to abrogate morphological alterations. These effects are discussed in light of potential clinical applications of antibody combinations.

Results

The growth-inhibitory effects of anti-HER2 monoclonal antibodies and their combination are reflected *in vitro*

We previously generated a battery of anti-HER2 mAbs and reported that unlike single mAbs, specific combinations of our mAbs were able to persistently eliminate HER2-overexpressing tumors in mice (Friedman *et al.*, 2005; Ben-Kasus *et al.*, 2009). Internalization and degradation induced by combinations of mAbs targeting the same receptor can contribute to therapeutic efficacy, especially when one antibody of the pair prevents receptor heterodimerization (Ben-Kasus *et al.*, 2009; Scheuer *et al.*, 2009). As the

proposed mechanism involves no immune effector cells, it is conceivable that the cooperative action of antibody combinations would be reflected *in vitro*, especially when applied on three-dimensional (3D) structures preserving structural and functional features of epithelial organs. To this end, our initial analyses tested the effects of different anti-HER2 therapeutics on T47D and BT474 breast cancer cells, grown either in 2D or 3D configurations (Figure 1). Cell viability assays performed on monolayers showed that the humanized antibody trastuzumab caused moderate reductions in cell proliferation (Figure 1a). In comparison, similar or more limited reductions were observed with our murine mAbs N12 and 431, which target distinct epitopes, including the dimerization site of HER2 (Klapper *et al.*, 1997; Yip *et al.*, 2001). Strikingly, we observed a more extensive reduction (42%) by the combination of mAbs N12 and 431 ($P=0.008$ for T47D cells, Student's paired t -test; Figure 1a). Similarly, enhanced growth-inhibitory effects were observed when another breast cancer cell line, MCF7, was used (Supplementary Figure S1). It is notable that MCF7 cells express relatively low levels of HER2, raising the possibility that the combination of mAbs sensitizes cells that express low levels of HER2 toward monoclonal antibodies. Using the same assay, we found that lapatinib reduced viability of T47D cells in a dose-dependent manner, reaching 42% at 250 nM ($P=0.01$; Figure 1b). Thus, a combination of two antibodies strongly inhibits growth of mammary tumor cells, and a kinase inhibitor is similarly potent.

Next, we monitored antibody effects on the average size of T47D spheroids ($n=80$) grown in 3D cultures (Figure 1c and Supplementary Figure S2). T47D spheroids were grown without and with neuregulin-beta1 (NRG), and from day 4 they were treated with lapatinib, trastuzumab, single murine mAbs or a combination. Notably, this analysis indicated that only the combination of mAbs induced a statistically significant ($P=0.0008$) effect on spheroid size. Neither NRG alone nor each single mAb elicited statistically significant alterations, although we noted positive and negative trends, respectively. Similar analyses of EGF-treated 3D structures formed by two additional mammary cell lines, SKBR3 and BT474, which highly and moderately overexpress HER2, respectively, suggested that the effect of antibody combination is general, rather than cell line specific (Supplementary Figure S2). Once again, only the combination of two mAbs resulted in statistically significant shrinking of spheroids, reinforcing the notion that antibody-induced morphogenic effects may not be effectively induced by each mAb alone, but they require cooperative actions of two mAbs.

Overexpression of HER2 enhances the growth-inhibitory effects of an antibody combination in a mammary model cell line

MCF10A cells are spontaneously immortalized, normal breast epithelial cells of human origin. This cell system and 3D derivative structures have been extensively used to analyze effects of HER2 and EGFR. For example, activation of HER2, but not of EGFR, led to re-initiation of intraluminal proliferation within 3D spheroids of MCF10A cells (Muthuswamy *et al.*, 2001). On the other hand, heterodimers of HER2 and EGFR are able to induce invasive growth of HER2-overexpressing MCF10A spheroids (Zhan *et al.*, 2006). Using retroviral vectors, we previously established a derivative of MCF10A cells that co-expresses HER2 and the green fluorescent protein (Chaluvally-Raghavan Pradeep *et al.*, manuscript submitted for publication). Employing this experimental system, along with control MCF10A cells expressing green fluorescent protein alone, we found that HER2-overexpressing spheroids protrude invasive arms into the surrounding extracellular matrix upon EGF stimulation (Chaluvally-Raghavan Pradeep *et al.*, manuscript submitted for publication). Hence, we assumed that MCF10A-HER2 cells may reflect the ability of antibody combinations to alter morphology and invasiveness of 3D mammary structures.

As a first step, we used monolayers of MCF10A-HER2 cells to examine lapatinib, as well as mAbs N12, 431 and their combination, in a cell viability assay (Figure 2). As observed when using mammary cancer cells (Figure 1a and Supplementary Figure S1), the combination of mAbs was able to reduce viability to a larger extent than each antibody alone. Notably, the inhibitory effect of the combination appeared already at lower concentrations compared with each single mAb, in correspondence with the ability to saturate HER2 binding (Ben-Kasus *et al.*, 2009). In addition, it is important noting that the effects of both lapatinib and the antibody combination on inhibition of cell viability were more pronounced in MCF10A-HER2 cells than in the parental cells. In conclusion, the cooperative inhibitory effects of mAbs to HER2 may be extended to a model cellular system overexpressing HER2. It is nevertheless imperative noting that MCF10A cells, whose HER2 level is low, also displayed inhibition by the mAb combination, suggesting that the mixture may sensitize low expressors of HER2, such as MCF10A and MCF7 cells.

To quantify the effect of mAb combination on cell viability, we calculated the area between the horizontal line corresponding to 100% viability and the actual curves (piecewise linear function joining the observation points). This area was denoted AUC (area under the curve) in the following description (see Supplementary Materials and methods). The calculated AUC values are shown in Supplementary Figure S3A. It is clear that adding a second mAb significantly increased AUC, especially in T47D and in MCF10A-HER2 cells. Next, we calculated for each cell line the percentage of increase of AUC of the mAb combination, beyond additive effects of single mAbs (Supplementary Figure S3B). A synergistic effect of the mAb combination was observed in all three cell lines, with the strongest effect observed in T47D cells. Finally, the observed viability in the MCF10A-HER2 cell line was modelled using a Michaelis–Menten equation with two parameters (see Supplementary Materials and methods for details). We compared the values of the model parameters E_m (lowest overall cell viability reached by the specific treatment) and K_d (concentration resulting in half of the maximal effect) for the single and combined administration of N12 and 431 (Supplementary Figure S3C). The results indicated that relatively low concentrations of the mAb combination elicited similarly potent effects to that induced by much higher concentrations of the single mAbs. Altogether, these calculations clearly attribute a synergistic inhibitory effect to the combination of two mAbs to HER2.

Anti-HER2-targeted therapies are able to reverse EGF-induced invasive phenotypes of MCF10A-HER2 spheroids

As a prelude to testing morphogenic effects of mAb combinations, MCF10A-HER2 spheroids were grown with EGF (20 ng/ml), and from day 4 onward they were treated with a single mAb, N12 or 431, or with their combination. When analyzing average spheroid size, we observed that the mixture of two mAbs exerted a significantly stronger effect on the reduction of average spheroid size (Supplementary Figure S4A; $P=4 \times 10^{-5}$ for the combination vs N12, $P=0.002$ for the combination vs mAb 431; $n>50$ for each analysis). This observation is reminiscent of the results we obtained with NRG-treated breast cancer cells, implying that spheroid size may serve as an indicator of therapeutic efficacy. The detailed microscopic analysis, which also included lapatinib and trastuzumab, is shown in Figure 3. In contrast to MCF10A spheroids, which displayed a lumen in the un-stimulated state, luminal filling occurred in untreated MCF10A-HER2 spheroids, confirming the ability of an overexpressed HER2 to increase luminal proliferation (Debnath *et al.*, 2002). Importantly, EGF had no detectable effect on the outer shape of MCF10A spheroids, but in MCF10A-HER2 spheroids EGF was able to induce outgrowths that invaded into the surrounding matrix (Supplementary Figure 3A), in line with a previous report (Zhan *et al.*, 2006). All drug treatments shown in Figure 3b were able to inhibit ligand-induced formation of invasive structures in MCF10A-HER2 spheroids (note the 20-fold lower concentration of

the mAb combination compared with trastuzumab). Alongside with inhibition of outgrowths, upon long incubation with the drugs, a lumen appeared in all treatment groups. In conclusion, luminal filling is propelled by HER2 overexpression, as previously shown using chimeric HER2 molecules (Muthuswamy *et al.*, 2001). On the other hand, formation of invasive structures is driven by EGF, but both phenotypes can be reversed to variable extents by anti-HER2 agents, such as a kinase inhibitor and an mAb combination.

Computational image analyses indicate that stimulation with EGF alters morphological parameters and reduces intraluminal death of MCF10A-HER2 spheroids

Owing to the subtle effects of HER2 overexpression and EGF treatment on spheroid morphology, we applied a home-written quantitative image analysis software using photomicrographs captured by confocal microscopy. Briefly, intraluminal cell death and invasive extensions from spheroid surfaces were evaluated as follows: the borders of the spheroids were identified by a threshold (Figure 4a). A higher threshold level (set as a constant fraction of the intensity inside the spheroid) identified internal details (for example, low fluorescence area due to cell death in the lumen). The fractions of non-apoptotic luminal areas from the total spheroid area were calculated ('Core Factor'), to depict the inner structures and reflect spaces. The ratio of spheroid's area to hull area (cell-to-hull ratio, CTH; Figure 4b) assessed the dispersion of the outer border of spheroids. In other words, CTH indicate how smooth and convex are the outlines of spheroids. Another parameter that evaluates the smoothness of spheroids surface, 'Solidity', measured the ratio between spheroid area and spheroid perimeter (Figure 4b).

Control MCF10A spheroids, which were cultured for 15 days without or with EGF (20 ng/ml), displayed no significant differences when the values of Core Factor and CTH were compared (Figures 5a and c). In contrast, MCF10A-HER2 spheroids displayed a significant effect of EGF on both the Core Factor ($P=0.003$; Figure 5b) and CTH ($P=0.004$; Figure 5d) on day 15. This difference is not yet detectable at day 10 (results not shown), indicating that the apoptosis-resistant, invasive phenotype develops over time following stimulation of HER2-overexpressing spheroids with EGF.

A combination of two mAbs better than single antibodies reverses EGF-induced changes of CTH and Core Factor in a model cellular system overexpressing HER2

To quantify the effects of EGF- and anti-HER2-targeted treatments of MCF10A-HER2 spheroids, the 3D structures were treated with lapatinib, mAb N12, mAb 431 or a mAb combination, and cross-section photomicrographs were captured on day 15 (Figure 6). The results we obtained clearly indicated that the mAb combination was able to more strongly reverse the effect of EGF on the Core Factor than each antibody alone (combination of antibodies vs mAb N12 alone: $P=0.0002$; combination vs mAb 431 alone: $P=0.0001$). This applied also to CTH: the mAb combination was superior to single antibody treatments in reversing the EGF-induced invasive phenotype (combination vs mAb N12: $P=0.02$; combination vs mAb 431: $P=0.04$). As expected, lapatinib (100 nM) was able to significantly reverse the EGF-induced phenotype both for Core Factor ($P=0.01$) and CTH ($P=0.03$). In conclusion, the computational image analyses we performed on multiple 3D structures firmly established the ability of an antibody combination to restore regular shape (CTH and Solidity) and increase intraluminal cell death (Core Factor).

A combination of monoclonal antibodies to HER2 transforms 3D cancer cell structures into smaller spheroids

To extend the image analyses to breast cancer cells, T47D cells were grown for 4 days in the absence or presence of NRG (20 ng/ml). Thereafter, media containing the single mAbs, or their combination, along with NRG, were added and refreshed every 4 days. Microscopic

inspection indicated extensive emergence of very small spheroids with patchy lumen on treatment with a combination of mAbs (data not shown and Figure 1c). The image analyses shown in Figure 7 reflect this transformation by a dramatic reduction in the cross-section spheroid areas. Despite reduced size, internal hollow areas were detectable. In analogy to MCF10A-HER2 cells, the combination of monoclonal antibodies, better than each mAb alone, was able to extend these regions, which reflects increased intraluminal cell death (measured as Core Factor; Figure 7a). Likewise, the effect of the mAb combination on the other two morphological parameters, CTH and Solidity, displayed statistically significant differences when compared with each mAb alone, and also when compared to untreated 3D cultures of T47D cells (Figures 7b and c). Notably, the effects on spheroid morphology were not observed on day 10 (data not shown), indicating that the mixture of mAbs, unlike single mAbs, can transform preformed structures. Conceivably, NRG-mediated activation of HER2 heterodimers is required for the maintenance of large and irregular tumor spheroids. Hence, when HER2 signaling is disrupted by a combination of mAbs, spheroids undergo transformation that normalizes their morphology.

In the next step, we directly addressed the ability of an antibody combination to negate two major actions of HER2: inhibition of apoptosis and enhancement of invasion. To this end, we treated spheroids of HER2-overexpressing SKBR3 cells with a combination of mAbs N12 and 431, and assayed cell death using propidium iodide. The results of this experiment confirmed enhanced ability of the mAb combination to induce cell death within spheroids of breast cancer cells (Supplementary Figure S5). Employing the same cell line and an invasion assay that tests migration through a porous, Matrigel-coated filter, we also verified an inhibitory effect of the mAb combination on invasion of cancer cells naturally overexpressing HER2 (Supplementary Figure S6). Interestingly, both the apoptosis and the invasion assays detected significant activities of each mAb when applied alone, but the effects of the combination were stronger and statistically more significant in both assays.

In summary, when tested in the conventional configuration of cellular monolayers, the combination of two anti-HER2 antibodies, of which mAb 431 is directed against the heterodimerization site, more potently than the respective single mAbs inhibited proliferation of all mammary cell lines we tested. Although the 3D configuration of cell cultures reflected this growth-inhibitory effect by a reduced spheroid size, 3D structures grown in extracellular matrix displayed more subtle morphogenic effects of the combination of mAbs: In MCF10A-HER2 cells, the dual antibody treatment enhanced intraluminal apoptosis while negating the invasion-promoting action of growth factors (Figures 3 and 6), whereas in T47D cells the mixture of two mAbs transformed the invasive structures into relatively small lumen-containing particles (Figure 7). Altogether, these results imply that the synergistic cellular effects of the mAb combination might be owing to increased inhibition of the action of HER2 as a signal amplifier of the receptors for EGF and NRGs.

Discussion

Although HER2 is aberrantly expressed in substantial fractions of a large spectrum of carcinomas (Schneider *et al.*, 1989; Yoshida *et al.*, 1989; Weiner *et al.*, 1990; Hou *et al.*, 1992; Xia *et al.*, 1997), its overexpression in breast cancer is the best understood, and has already been translated to therapy (Hynes and MacDonald, 2009). Nevertheless, the roles HER2 plays in breast cancer are incompletely understood: while approximately a quarter of mammary tumors overexpress HER2, this receptor kinase molecule is present in exaggerated numbers in >45% of ductal carcinoma *in situ*, pre-invasive lesions. The putative critical transition from ductal carcinoma *in situ* to invasive tumors involves breakdown of the encasing basement membrane, and acquisition of a motile phenotype (Hu *et al.*, 2008). 3D cultures of mammary cells helped understanding that HER2 overexpression is essential

for lumen filling with proliferating cells, which evade anoikis (Muthuswamy *et al.*, 2001). However, what enables HER2 to trigger breakdown of the basement membrane remains unclear. Previous studies identified EGF-like ligands (Zhan *et al.*, 2006) and transforming growth factor- β (Seton-Rogers and Brugge, 2004; Ueda *et al.*, 2004) as potential promoters.

In vitro models of the transition must encompass processes influenced by HER2, such as breakdown of tissue architecture, uncoupling of adhesive interactions (Guo *et al.*, 2006) and disruption of epithelial polarity (Aranda *et al.*, 2006). Our study employed 3D models of the transition to invasive cancer, with the goal of testing interceptors of HER2 (Baselga *et al.*, 2009). Two arms were employed: the cancer cell arm examined the ability of drugs to control 3D structures, and the other arm employed an HER2-overexpressing derivative of non-malignant mammary cells, MCF10A, and addressed relations to expression levels of HER2. As expected, experiments performed on monolayers consistently showed the ability of an antibody combination to inhibit the proliferation-promoting action of HER2, but only the 3D format provided insights into HER2's morphogenic functions. Thus, the combination of mAbs, unlike single treatments, synergistically inhibited cell proliferation and reduced the size of spheroids (Figures 1a and c, Figure 2 and Supplementary Figure S2). On the other hand, the mixture of mAbs normalized the outer border, partly cleared luminal spaces (Figures 3 and 6) and disintegrated 3D structures of cancer cells. These observations are consistent with previous *in vitro* (Nahta *et al.*, 2004) and animal studies (Ben-Kasus *et al.*, 2009; Scheuer *et al.*, 2009). Yet, another study reported enhanced HER2 activation in 3D formats (Pickl and Ries, 2009). In contrast with mAbs, treatment with growth factors not only induces proliferation, but also inhibits luminal cell death and promotes outgrowths in model spheroids (Figure 5), implying that mAb combinations negate the action of growth factors. In line with this scenario, resistance to trastuzumab has been correlated with enhanced expression of EGFR and secretion of several EGF-like ligands (Ritter *et al.*, 2007).

Conceivably, when two anti-HER2 antibodies are combined, they inhibit both actions of HER2, namely intraluminal proliferation and invasion across the basement membrane. The latter is likely propelled by growth factors (Zhan *et al.*, 2006). If correct, our model attributes to HER2 interceptors the ability to block both intraluminal proliferation and, more importantly, the critical transition from *in situ* to invasive breast carcinoma, a process controlled by the stroma (Hu *et al.*, 2008). Another model supported by our studies refers to the mechanism of immunotherapies targeting receptors like HER2. Antibody-mediated recruitment of natural killer lymphocytes to cancer cells emerged from animal studies (Clynes *et al.*, 2000), but several non-immunological mechanisms have been described (reviewed by Ben-Kasus *et al.* (2007)). For example, we previously proposed that large receptor-antibody complexes are generated on the cell surfaces when mAbs engaging different epitopes are used (Friedman *et al.*, 2005). Consequently, these complexes collapse into the cytoplasm and they are eventually subjected to degradation in lysosomes. As our models employed no immune cells, the results presented in this study favor the involvement of non-immunological mechanisms.

In summary, combining two antibodies directed against different epitopes of HER2 emerges from this and other recent studies as a promising strategy to target mammary tumors expressing variable levels of HER2. Combining two mAbs presents a feasible therapeutic approach. Initial clinical applications using trastuzumab and pertuzumab lend support to the feasibility of antibody combinations, and raise the intriguing possibility that this scenario can overcome resistance to a single antibody (Baselga *et al.*, 2009). The 3D models and morphometric parameters we studied herein provide useful insights into the effects of therapeutic antibodies, and may permit selection of optimal mAb combinations.

Materials and methods

Reagents and cells

Unless indicated, materials were purchased from Sigma (St Louis, MO, USA) and antibodies from Santa Cruz Biotechnology (Santa Cruz, CA, USA). MCF10A cells were grown in Dulbecco's modified Eagle's/F12 medium containing 5% horse serum, 10 $\mu\text{g/ml}$ insulin, 0.1 $\mu\text{g/ml}$ cholera toxin, 0.5 $\mu\text{g/ml}$ hydrocortisone, 10 ng/ml EGF and 100 U/ml penicillin/streptomycin. BT474 and SKBR3 cell lines were maintained in Dulbecco's modified Eagle's medium containing L-glutamine, and T47D cells were cultured in RPMI medium supplemented with insulin (10 $\mu\text{g/ml}$). MCF10A-HER2 and MCF10A cells stably expressing green fluorescent protein were established by transfection and selection (our manuscript submitted for publication). Lapatinib was obtained from LC Laboratories (Woburn, MA, USA). Trastuzumab was provided by Genentech (South San Francisco, CA, USA). Cetuximab was provided by Wolfgang Köstler, University Hospital of Vienna. Growth factor reduced Matrigel was obtained from BD Biosciences (Bedford, MA, USA). NRG was obtained from Prepro Tech Asia (Rocky Hill, NJ, USA). The Cell Proliferation Assay Kit using the XTT reagent was obtained from Biological Industries (Beit Haemek, Israel).

Immunofluorescence

Spheroids were grown in assay medium. On day 4, assay media containing the respective treatment were applied and changed on days 8, 12 and 15. Images were acquired using the Bio-Rad Radiance 2000 microscope (Oberkochen, Germany).

Morphogenesis assays

Eight-well chamber slides (BD Biosciences) were coated using 35 μl Matrigel solution per well. After regular growth in monolayers, cells were trypsinized and re-suspended in MCF10A Assay Medium supplemented with 2.5% Matrigel. The medium was refreshed every 4 days. In the case of treatment with mAbs, or with lapatinib, treatment was started on day 4.

Computational spheroid shape analysis

For the analysis of confocal microscopy images, we used a self-written image analysis software and Priism Image Visualization Environment (<http://www.msg.ucsf.edu/IVE/>). Acquired images were denoised by smoothing. Spheroids were defined by contiguous component binary segmentation, after setting a fixed threshold. Each spheroid was morphologically characterized by calculating area and perimeter (approximated by the number of border pixels), as well as the area and perimeter of the convex hull (the convex shape enclosing the spheroid segment). From these we calculated dimensionless parameters: Solidity = $(\text{area}/\pi)/(\text{Perim}/2\pi)$ and spheroid-to-convex hull area ratio (CTH). Both assume the value of 1 for a circle, and become smaller the more disperse the shape is; therefore, evaluating the invasive structures of the spheroids. In addition, a second, higher threshold level (specified as a fraction of the maximum intensity in each spheroid) allowed segmenting apoptotic regions within spheroids, owing to their lower fluorescence levels compared with live cells expressing the green fluorescent protein construct. Although the absolute value of the apoptotic area so determined depends on the chosen threshold level, the relative results for samples with different levels of apoptosis were correlated with visual comparisons. The parameters were evaluated for $n \sim 50$ spheroids under each condition, and statistically analyzed. ImageJ (<http://rsbweb.nih.gov/ij/>) was used for the analysis of spheroid area from phase contrast-photos.

Statistical analysis

For statistical analysis we used SPSS (Chicago, IL, USA). For statistical analysis of confocal imaging, we used >50 spheroids in each group. Comparison of means used the Mann–Whitney test. Student's paired *t*-test was used to compare spheroid areas from phase-contrast images for two groups ($n=30$).

Modeling and quantification of drug synergy

We applied parametric and non-parametric modeling methods to quantify drug synergy. The parametric method consisted of modeling survival data with a Michaelis–Menten function. Owing to the amount of data required by this method, we were only able to apply this method to HER2-MCF10 cells. Hence, we also analyzed the data by means of a non-parametric method. In this method, the data set was interpolated by a linear function for each viability curve. Thereafter, we calculated by means of a numerical integration the area between the curve $y=1$ (100% viability) and the interpolated curve. This area, reflecting drug activity, was calculated in the case of drug combination and compared with the case of single administrations (see Supplementary Materials and methods).

Supplementary Material

Refer to Web version on PubMed Central for supplementary material.

Acknowledgments

We thank members of our group for insightful comments. AE is supported by a post-doctoral fellowship of the Minerva Foundation. YY is the incumbent of the Harold and Zelda Goldenberg Professorial Chair, and MS is the incumbent of the W Garfield Weston Professorial Chair in Immunology. Our work is supported by a collaborative program between Centre Leon-Berard, Canceropole Lyon Auvergne Rhône-Alpes and the Weizmann Institute, as well as by grants from the National Cancer Institute (CA072981), the European Commission, the German–Israeli Project Cooperation (DIP/DFG), the Israel Cancer Research Fund, the Dr Miriam and Sheldon G Adelson Medical Research Foundation, the Kekst Family Institute for Medical Genetics, the Kirk Center for Childhood Cancer and Immunological Disorders, the Women's Health Research Center funded by Bennett–Pritzker Endowment Fund, the Marvelle Koffler Program for Breast Cancer Research, the Estate of John M, Lang and the MD Moross Institute for Cancer Research.

References

- Agus DB, Akita RW, Fox WD, Lewis GD, Higgins B, Pisacane PI, et al. Targeting ligand-activated ErbB2 signaling inhibits breast and prostate tumor growth. *Cancer Cell*. 2002; 2:127–137. [PubMed: 12204533]
- Aranda V, Haire T, Nolan ME, Calarco JP, Rosenberg AZ, Fawcett JP, et al. Par6-aPKC uncouples ErbB2 induced disruption of polarized epithelial organization from proliferation control. *Nat Cell Biol*. 2006; 8:1235–1245. [PubMed: 17060907]
- Baselga J. Targeting tyrosine kinases in cancer: the second wave. *Science*. 2006; 312:1175–1178. [PubMed: 16728632]
- Baselga J, Semiglazov V, van Dam P, Manikhas A, Bellet M, Mayordomo J, et al. Phase II randomized study of neoadjuvant everolimus plus letrozole compared with placebo plus letrozole in patients with estrogen receptor-positive breast cancer. *J Clin Oncol*. 2009; 27:2630–2637. [PubMed: 19380449]
- Ben-Kasus T, Schechter B, Lavi S, Yarden Y, Sela M. Persistent elimination of ErbB-2/HER2-overexpressing tumors using combinations of monoclonal antibodies: relevance of receptor endocytosis. *Proc Natl Acad Sci USA*. 2009; 106:3294–3299. [PubMed: 19218427]
- Ben-Kasus T, Schechter B, Sela M, Yarden Y. Cancer therapeutic antibodies come of age: targeting minimal residual disease. *Mol Oncol*. 2007; 1:42–54. [PubMed: 19383286]
- Citri A, Yarden Y. EGF-ERBB signalling: towards the systems level. *Nat Rev Mol Cell Biol*. 2006; 7:505–516. [PubMed: 16829981]

- Clynes RA, Towers TL, Presta LG, Ravetch JV. Inhibitory Fc receptors modulate *in vivo* cytotoxicity against tumor targets. *Nat Med.* 2000; 6:443–446. [PubMed: 10742152]
- Debnath J, Mills KR, Collins NL, Reginato MJ, Muthuswamy SK, Brugge JS. The role of apoptosis in creating and maintaining luminal space within normal and oncogene-expressing mammary acini. *Cell.* 2002; 111:29–40. [PubMed: 12372298]
- Drebin JA, Link VC, Greene MI. Monoclonal antibodies reactive with distinct domains of the neu oncogene-encoded p185 molecule exert synergistic anti-tumor effects *in vivo*. *Oncogene.* 1988; 2:273–277. [PubMed: 2451200]
- Friedman LM, Rinon A, Schechter B, Lyass L, Lavi S, Bacus SS, et al. Synergistic down-regulation of receptor tyrosine kinases by combinations of mAbs: implications for cancer immunotherapy. *Proc Natl Acad Sci USA.* 2005; 102:1915–1920. [PubMed: 15684082]
- Guo W, Pylayeva Y, Pepe A, Yoshioka T, Muller WJ, Inghirami G, et al. Beta 4 integrin amplifies ErbB2 signaling to promote mammary tumorigenesis. *Cell.* 2006; 126:489–502. [PubMed: 16901783]
- Hou L, Shi D, Tu SM, Zhang HZ, Hung MC, Ling D. Oral cancer progression and c-erbB-2/neu proto-oncogene expression. *Cancer Lett.* 1992; 65:215–220. [PubMed: 1355405]
- Hu M, Yao J, Carroll DK, Weremowicz S, Chen H, Carrasco D, et al. Regulation of *in situ* to invasive breast carcinoma transition. *Cancer Cell.* 2008; 13:394–406. [PubMed: 18455123]
- Hynes NE, MacDonald G. ErbB receptors and signaling pathways in cancer. *Curr Opin Cell Biol.* 2009; 21:177–184. [PubMed: 19208461]
- Kasprzyk PG, Song SU, Di Fiore PP, King CR. Therapy of an animal model of human gastric cancer using a combination of anti-erbB-2 monoclonal antibodies. *Cancer Res.* 1992; 52:2771–2776. [PubMed: 1349849]
- Klapper LN, Vaisman N, Hurwitz E, Pinkas-Kramarski R, Yarden Y, Sela M. A subclass of tumor-inhibitory monoclonal antibodies to ErbB-2/HER2 blocks crosstalk with growth factor receptors. *Oncogene.* 1997; 14:2099–2109. [PubMed: 9160890]
- Lemieux J, Clemons M, Provencher L, Dent S, Latreille J, Mackey J, et al. The role of neoadjuvant her2-targeted therapies in her2-overexpressing breast cancers. *Curr Oncol.* 2009; 16:48–57. [PubMed: 19862361]
- Muthuswamy SK, Li D, Lelievre S, Bissell MJ, Brugge JS. ErbB2, but not ErbB1, reinitiates proliferation and induces luminal repopulation in epithelial acini. *Nat Cell Biol.* 2001; 3:785–792. [PubMed: 11533657]
- Nahta R, Esteva FJ. Herceptin: mechanisms of action and resistance. *Cancer Lett.* 2006; 232:123–138. [PubMed: 16458110]
- Nahta R, Hung MC, Esteva FJ. The HER-2-targeting antibodies trastuzumab and pertuzumab synergistically inhibit the survival of breast cancer cells. *Cancer Res.* 2004; 64:2343–2346. [PubMed: 15059883]
- Pedersen MW, Jacobsen HJ, Koefoed K, Hey A, Pyke C, Haurum JS, et al. Sym004: a novel synergistic anti-epidermal growth factor receptor antibody mixture with superior anticancer efficacy. *Cancer Res.* 2010; 70:588–597. [PubMed: 20068188]
- Pickl M, Ries CH. Comparison of 3D and 2D tumor models reveals enhanced HER2 activation in 3D associated with an increased response to trastuzumab. *Oncogene.* 2009; 28:461–468. [PubMed: 18978815]
- Ritter CA, Perez-Torres M, Rinehart C, Guix M, Dugger T, Engelman JA, et al. Human breast cancer cells selected for resistance to trastuzumab *in vivo* overexpress epidermal growth factor receptor and ErbB ligands and remain dependent on the ErbB receptor network. *Clin Cancer Res.* 2007; 13:4909–4919. [PubMed: 17699871]
- Scheuer W, Friess T, Burtscher H, Bossenmaier B, Endl J, Hasmann M. Strongly enhanced antitumor activity of trastuzumab and pertuzumab combination treatment on HER2-positive human xenograft tumor models. *Cancer Res.* 2009; 69:9330–9336. [PubMed: 19934333]
- Schneider PM, Hung MC, Chiocca SM, Manning J, Zhao XY, Fang K, et al. Differential expression of the c-erbB-2 gene in human small cell and non-small cell lung cancer. *Cancer Res.* 1989; 49:4968–4971. [PubMed: 2569928]

- Seton-Rogers SE, Brugge JS. ErbB2 and TGF-beta: a cooperative role in mammary tumor progression? *Cell Cycle*. 2004; 3:597–600. [PubMed: 15107620]
- Slamon DJ, Clark GM, Wong SG, Levin WJ, Ullrich A, McGuire WL. Human breast cancer: correlation of relapse and survival with amplification of the HER-2/neu oncogene. *Science*. 1987; 235:177–182. [PubMed: 3798106]
- Spangler JB, Neil JR, Abramovitch S, Yarden Y, White FM, Lauffenburger DA, et al. Combination antibody treatment down-regulates epidermal growth factor receptor by inhibiting endosomal recycling. *Proc Natl Acad Sci USA*. 2010; 107:13252–13257. [PubMed: 20616078]
- Spiridon CI, Ghetie MA, Uhr J, Marches R, Li JL, Shen GL, et al. Targeting multiple Her-2 epitopes with monoclonal antibodies results in improved antigrowth activity of a human breast cancer cell line *in vitro* and *in vivo*. *Clin Cancer Res*. 2002; 8:1720–1730. [PubMed: 12060609]
- Ueda Y, Wang S, Dumont N, Yi JY, Koh Y, Arteaga CL. Overexpression of HER2 (erbB2) in human breast epithelial cells unmasks transforming growth factor beta-induced cell motility. *J Biol Chem*. 2004; 279:24505–24513. [PubMed: 15044465]
- Weiner DB, Nordberg J, Robinson R, Nowell PC, Gazdar A, Greene MI, et al. Expression of the neu gene-encoded protein (P185neu) in human non-small cell carcinomas of the lung. *Cancer Res*. 1990; 50:421–425. [PubMed: 1967224]
- Xia W, Lau YK, Zhang HZ, Liu AR, Li L, Kiyokawa N, et al. Strong correlation between c-erbB-2 overexpression and overall survival of patients with oral squamous cell carcinoma. *Clin Cancer Res*. 1997; 3:3–9. [PubMed: 9815530]
- Xia W, Mullin RJ, Keith BR, Liu LH, Ma H, Rusnak DW, et al. Anti-tumor activity of GW572016: a dual tyrosine kinase inhibitor blocks EGF activation of EGFR/erbB2 and downstream Erk1/2 and AKT pathways. *Oncogene*. 2002; 21:6255–6263. [PubMed: 12214266]
- Yarden Y, Sliwkowski MX. Untangling the ErbB signalling network. *Nat Rev Mol Cell Biol*. 2001; 2:127–137. [PubMed: 11252954]
- Yip YL, Smith G, Koch J, Dubel S, Ward RL. Identification of epitope regions recognized by tumor inhibitory and stimulatory anti-ErbB-2 monoclonal antibodies: implications for vaccine design. *J Immunol*. 2001; 166:5271–5278. [PubMed: 11290813]
- Yoshida K, Tsuda T, Matsumura T, Tsujino T, Hattori T, Ito H, et al. Amplification of epidermal growth factor receptor (EGFR) gene and oncogenes in human gastric carcinomas. *Virchows Arch B*. 1989; 57:285–290. [PubMed: 2570489]
- Zhan L, Xiang B, Muthuswamy SK. Controlled activation of ErbB1/ErbB2 heterodimers promote invasion of three-dimensional organized epithelia in an ErbB1-dependent manner: implications for progression of ErbB2-overexpressing tumors. *Cancer Res*. 2006; 66:5201–5208. [PubMed: 16707444]

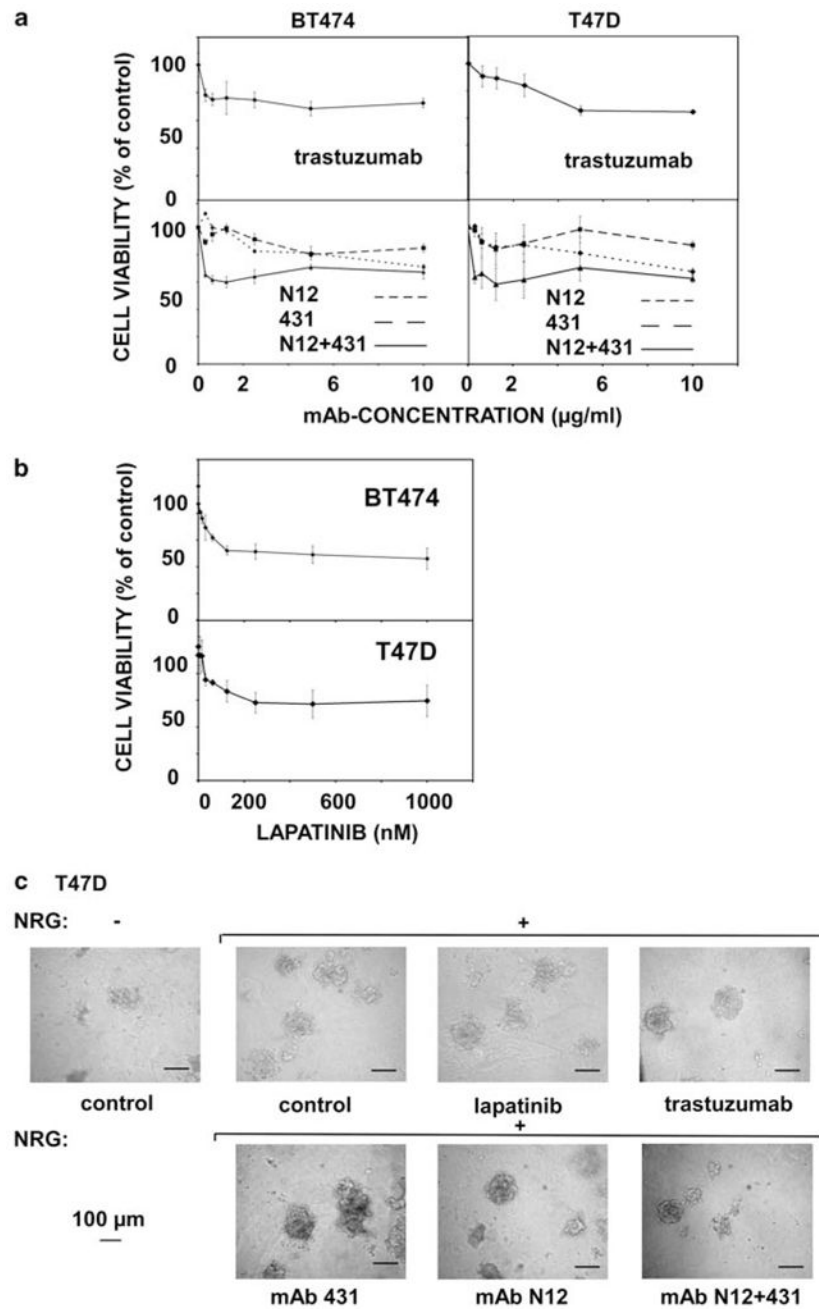


Figure 1. Growth-inhibitory effects of anti-HER2 monoclonal antibodies and a tyrosine kinase inhibitor on T47D and BT474 breast cancer cells grown in monolayers and in 3D cultures. **(a, b)** Cells were cultured for 24 h and then treated with increasing drug concentrations for 48 h, as indicated. Cell viability is shown as the percentage of control, untreated cells. The experiment was repeated thrice. Averages \pm s.d. (bars) of triplicates are shown. **(c)** T47D cells were grown in a natural extracellular matrix (Matrigel) to form spheroids. NRG (20 ng/ml) was added at time zero, whereas mAbs were added at day 4. The respective media were refreshed every 4 days. Shown are representative phase-contrast photos of T47D spheroids (taken at day 15). Bars, 100 μ m.

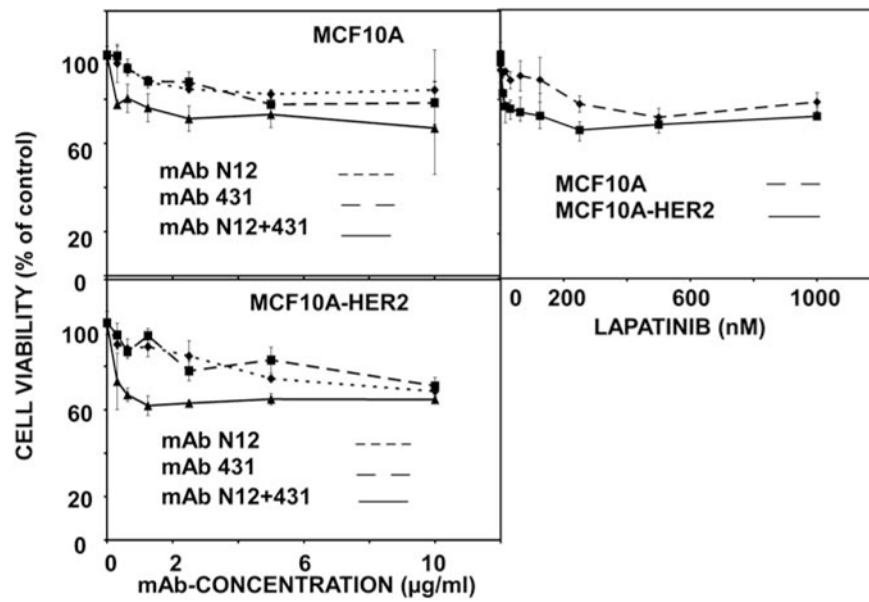


Figure 2.

Effects of anti-HER2 antibodies and their combination on the viability of MCF10A and MCF10A-HER2 cells. Sub-confluent monolayers of MCF10A and MCF10A-HER2 cells were grown in 96-well plates for 24 h, and then treated with increasing concentrations of mAbs or lapatinib. Cell metabolism (XTT assay) was determined 48 h later, and the results presented as average \pm s.d. (bars) of triplicates. The experiment was repeated three times.

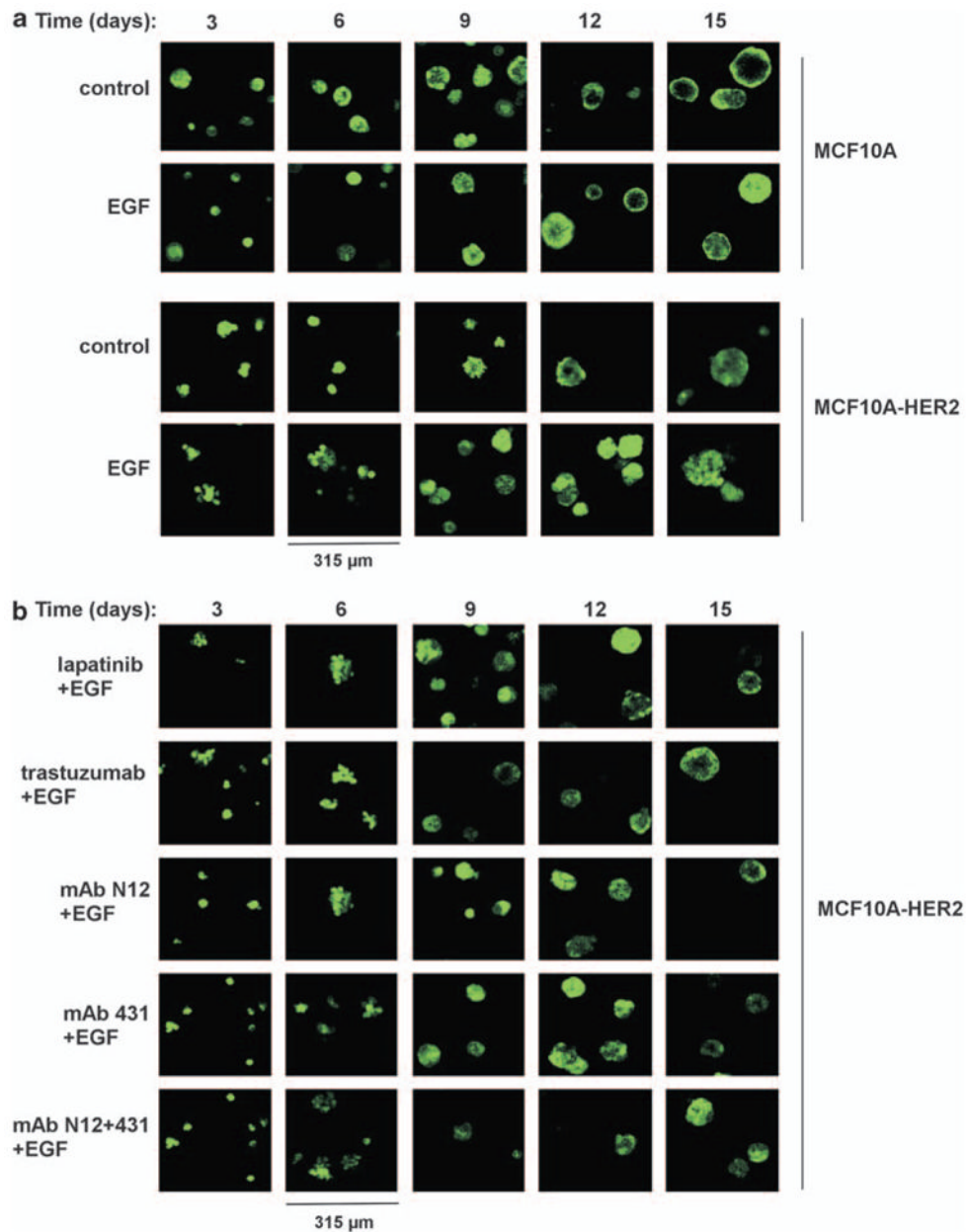


Figure 3. EGF induces an invasive phenotype in MCF10A-HER2 spheroids, and anti-HER2-targeted therapies are able to reverse this phenotype. MCF10A (**a**) and MCF10A-HER2 (**a, b**) cells were cultured for 4 days in an extracellular matrix (Matrigel), in the absence or presence of EGF (20 ng/ml). This was followed by media replacement for drug-containing media. The following drugs were used: trastuzumab (12.5 μ g/ml), lapatinib (100 nM), N12 (0.625 μ g/ml), 431 (0.625 μ g/ml) or a mixture of mAbs N12 and 431 (0.625 μ g/ml total concentration). Photomicrographs taken after the indicated time intervals are shown.

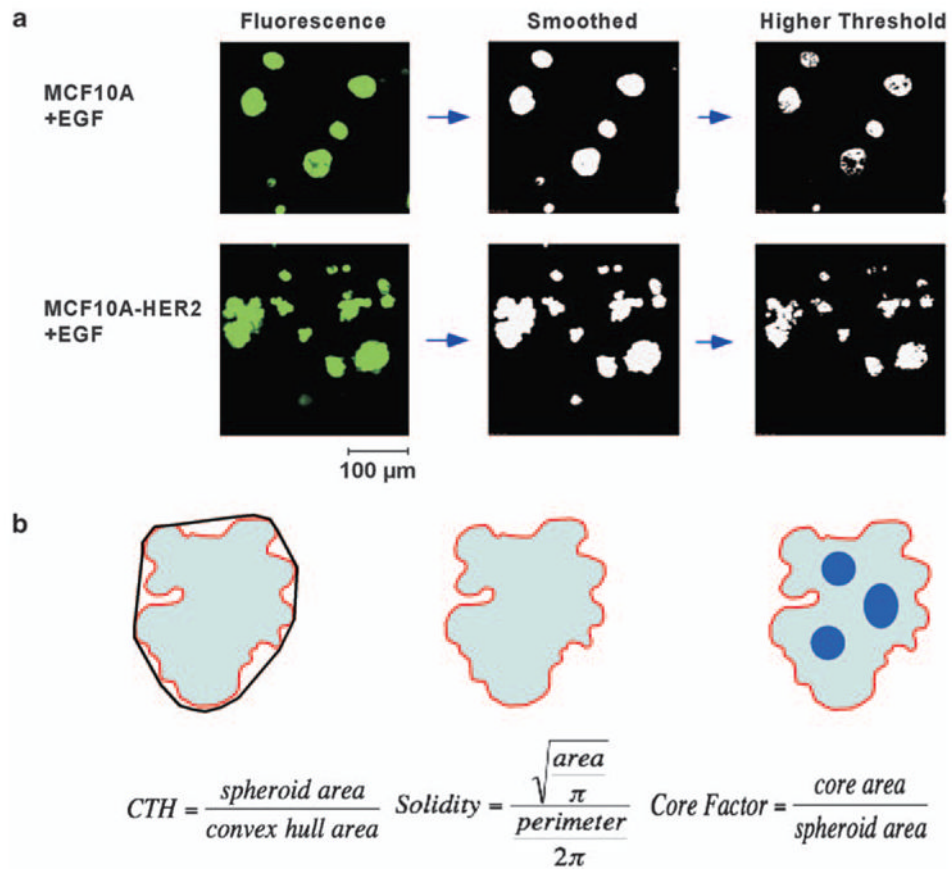


Figure 4. Computational image analysis of mammary cell spheroids. **(a)** Schematic representation of the processing of fluorescent images. Confocal images of spheroids of EGF-treated MCF10A and MCF10A-HER2 cells are shown as an example. Acquired images were smoothed and thresholded. **(b)** The convex hull is outlined and CTH and Solidity are calculated. The Core Factor is calculated by comparing images at different thresholds.

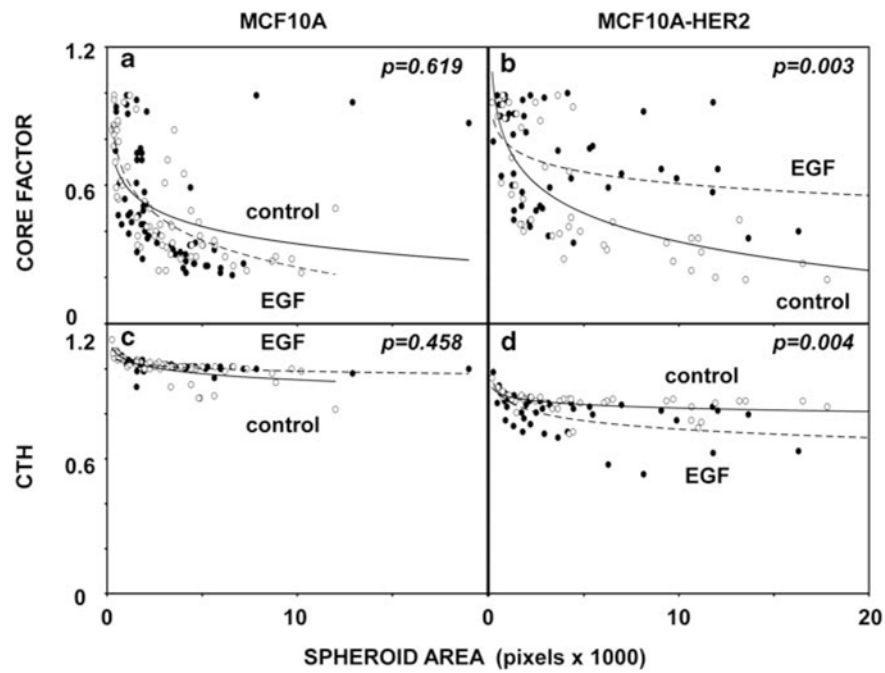


Figure 5. Stimulation with EGF significantly alters the shape and reduces intraluminal death of MCF10A-HER2 cells grown as spheroids. MCF10A (**a, c**) and MCF10A-HER2 (**b, d**) cells were grown as spheroids without (open circles) or with EGF (20 ng/ml; closed circles) in a 3D matrix. Spheroids formed by day 15 were analyzed. The values of Core Factor and CTH were calculated for each spheroid and presented in scatter plots, relative to cross-section areas. The respective *P*-values ($n > 50$) were calculated using the Mann–Whitney test and SPSS.

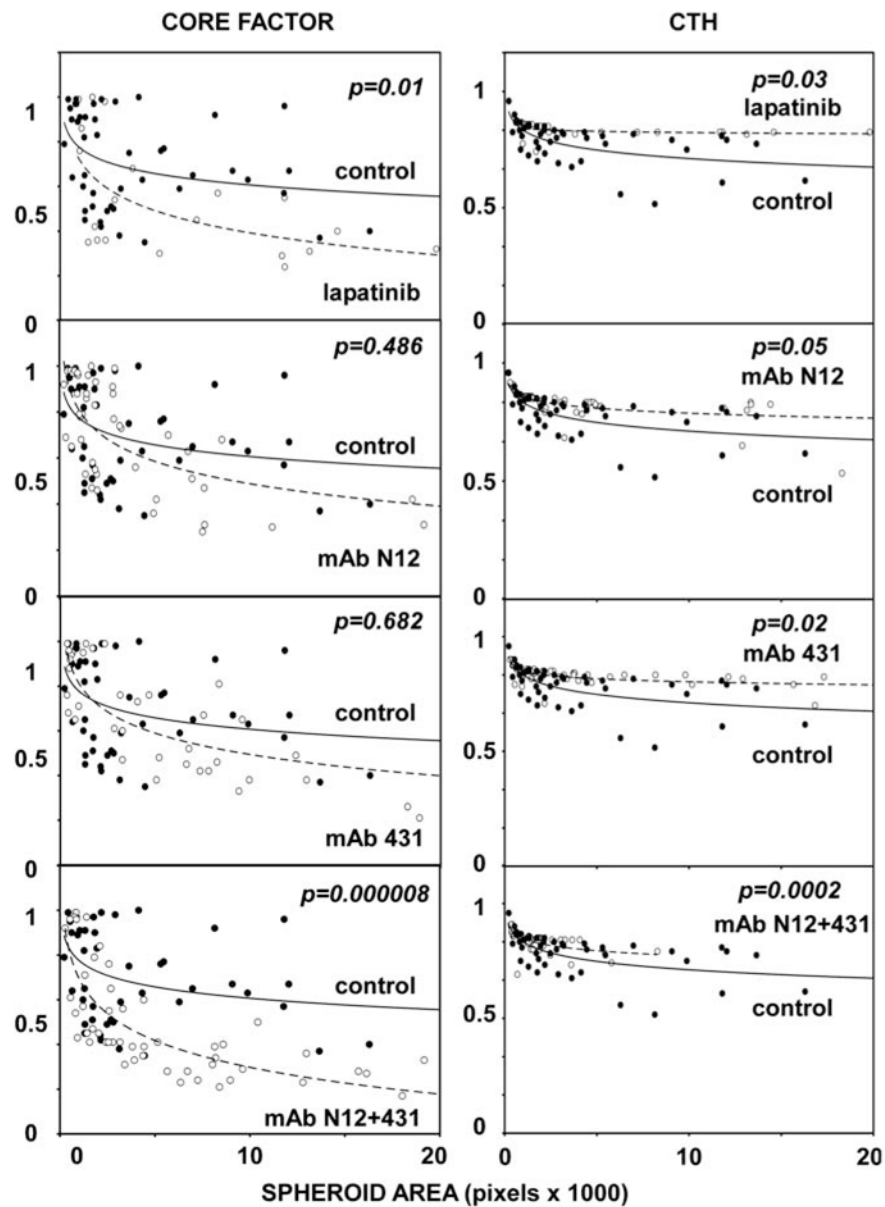


Figure 6.

A combination of mAbs reverses EGF-induced changes of CTH and Core Factor more potently than single antibodies. MCF10A-HER2 cells were cultured as in Figure 5 in the presence of EGF (20 ng/ml), except that single mAbs or their combination were added at day 4, and their effects tested at day 15. Total antibody concentration in each group was 2.5 $\mu\text{g/ml}$ in the Core Factor analysis and 10 $\mu\text{g/ml}$ in the CTH analysis. Lapatinib concentration was 100 nM in both analyses. The control is indicated by solid circles. *P*-values were calculated using the Mann–Whitney test and SPSS ($n > 50$).

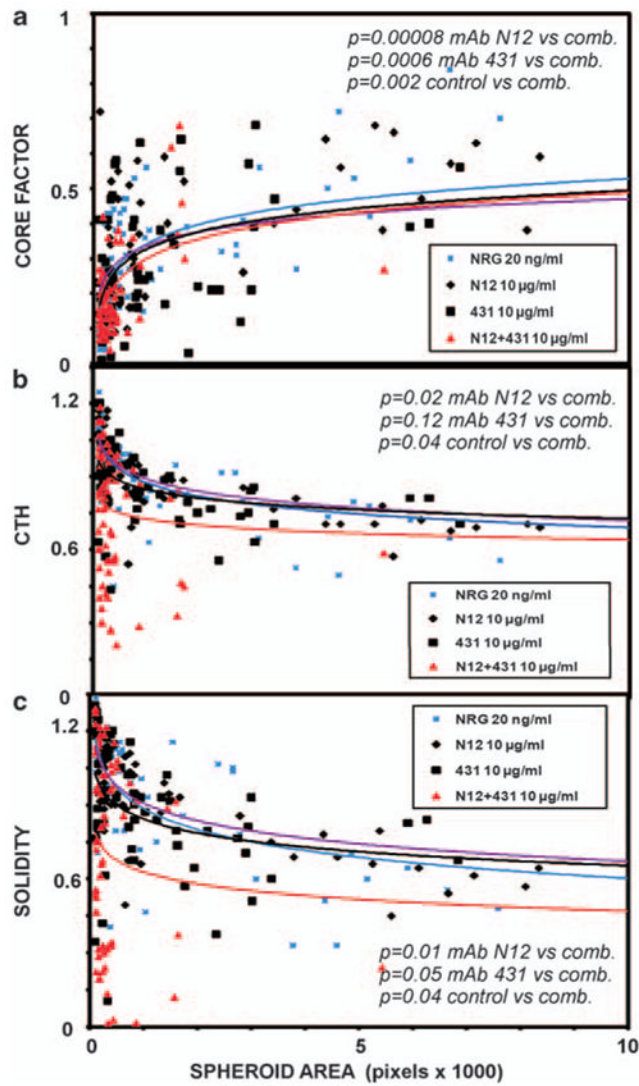


Figure 7.

A combination of monoclonal antibodies to HER2 is able to disrupt integrity of T47D spheroids. T47D cells were grown for 15 days in Matrigel in the presence of NRG (20 ng/ml; added at day 1), single mAbs or their combination (comb.; added at day 4), as indicated. Each mAb was used at 10 µg/ml or at 5 µg/ml when combined with the other mAb. Scatter plots were obtained from 80 spheroids for each group (two independent experiments). The indicated *P*-values were calculated with SPSS using the Mann–Whitney test. **(a)** Core factor; **(b)** CTH; **(c)** Solidity.